Letter of Intent

Pion-induced phi meson production on the proton

Takatsugu Ishikawa[a] and Hiroaki Ohnishi

Research Center for Electron Photon Science (ELPH),

Tohoku University, Sendai, Miyagi 982-0826, Japan

Kazuya Aoki, Kyoichiro Ozawa, Shin'ya Sawada, Hitoshi Takahashi, and Yuhei Morino

Institute of Particle and Nuclear Studies (IPNS),

High Energy Accelerator Research Organization (KEK), Tsukuba, Ibaraki 305-0801, Japan

Wen-Chen Chang

Institute of Physics, Academia Sinica, Taipei 11529, Taiwan

Tomoaki Hotta, Hiroyuki Noumi, Kotaro Shirotori, and Natsuki Tomida

Research Center for Nuclear Physics (RCNP),

Osaka University, Ibaraki, Osaka 567-0047, Japan

Masashi Kaneta

Department of Physics, Tohoku University, Sendai, Miyagi 980-8578, Japan

Megumi Naruki

Department of Physics, Kyoto University, Kyoto, Kyoto 606-8502, Japan

Satoshi Yokkaichi

Nishina Center for Accelerator-Based Science,

Institute of Physical and Chemical Research (RIKEN), Wako, Saitama 351-0198, Japan

Abstract

A resonance-like behavior (bump) peaked at around 2.2 GeV has been observed in the differential cross section $d\sigma/dt$ at $t = -|t|_{\rm min}$ as a function of the incident photon energy E_γ for ϕ photoproduction on the proton ($\gamma p \to \phi p$). Currently, the origin of this bump is not clear. The $d\sigma/dt$ at a fixed E_γ in $\gamma p \to \phi p$ shows a strong exponential behavior from the threshold, suggesting ϕ photoproduction is insensitive to s-channel ϕ-nucleon resonances. To reveal the origin of this bump, we measure the angular differential cross section $d\sigma/d\Omega$ at incident pion momenta ranging from 1.6 to 2.4 GeV/c for pion-induced phi meson production on the proton ($\pi^- p \to \phi n$). In this measurement, we plan to use secondary pions ($\approx$ 10 kHz) delivered at the high-p beamline with a 400-W loss of the primary proton beam at the Lambertson magnet. We expect to obtain several hundred ϕ-produced events at a fixed incident momentum in 10-days measurement by utilizing the spectrometer magnet for the E16 experiment and the combined detector system for the E16 and E50 experiments.

PACS numbers: 13.60.Le, 14.20.Gk, 13.75.Gx

[a] Spokesperson: ishikawa@lns.tohoku.ac.jp

I. INTRODUCTION

Hadrons are composite particles consisting of quarks and gluons. The strong interaction between them is provided in the fundamental theory, quantum chromodynamics (QCD). Nevertheless, the dynamics of hadrons is difficult to be described from the interaction between quarks and gluons. Neither quarks nor gluons are direct effective degrees of freedom (building blocks) of hadrons. Instead, dressed quarks (constituent quarks) and pions (Nambu-Goldstone bosons), emerging from the chiral symmetry breaking, play a role of a building block. Several models incorporating them well-reproduce not only the properties of the ground-state hadrons [1, 2] but also the important features of the interaction between nucleons (nuclear force) [3, 4]. Simply describing quarks as constituent quarks, familiar hadrons are classified into mesons containing a quark-antiquark pair ($q\bar{q}$) and baryons containing three quarks (qqq). And excited hadrons are considered as radial and orbital excitations of the ground-state hadrons. However, disagreement has been recognized between experimental results and theoretical calculations for highly-excited (or high-mass) hadrons. Especially the so-called exotic hadrons receive a particular interest since they are comprised of more than three quarks.

Recently, hidden-charm P_c baryons, $P_c(4312)^+$, $P_c(4440)^+$, and $P_c(4457)^+$, are reported by the LHCb collaboration, which are observed in the $J/\psi p$ invariant-mass distributions for the $\Lambda_b \to J/\psi p K^-$ decay [5, 6] as shown in Fig. 1. These P_c baryons could be a spatially-compact pentaquark object ($qqqq\bar{q}$) and/or a meson-baryon molecule-like state ($\Sigma_c^+ \bar{D}^0$ or $\Sigma_c^+ \bar{D}^{*0}$). If a P_c baryon really exists, it should show up independently of the initial state of reactions. The GlueX collaboration measures the total cross section as a function of the incident photon energy for J/ψ photoproduction on the proton ($\gamma p \to J/\psi p$) [7]. No peaks are observed corresponding to the P_c baryons reported by the LHCb collaboration. There is a possibility that the small branching ratio of $P_c \to J/\psi p$ makes it difficult to observe them in photoproduction. Still not definitely settled is what is the structure of the P_c baryons [8–10].

The J/ψ meson consists of almost pure $c\bar{c}$, while the phi meson (ϕ) consists of almost pure $s\bar{s}$. The Okubo-Zwieg-Iizuka (OZI) rule makes the interaction of these mesons to the nucleon weak owing to little admixture of $c\bar{c}$ or $s\bar{s}$ in the nucleon wave function. Thus, the resonances have not been considered between ϕ (J/ψ) and the nucleon. However, a similar

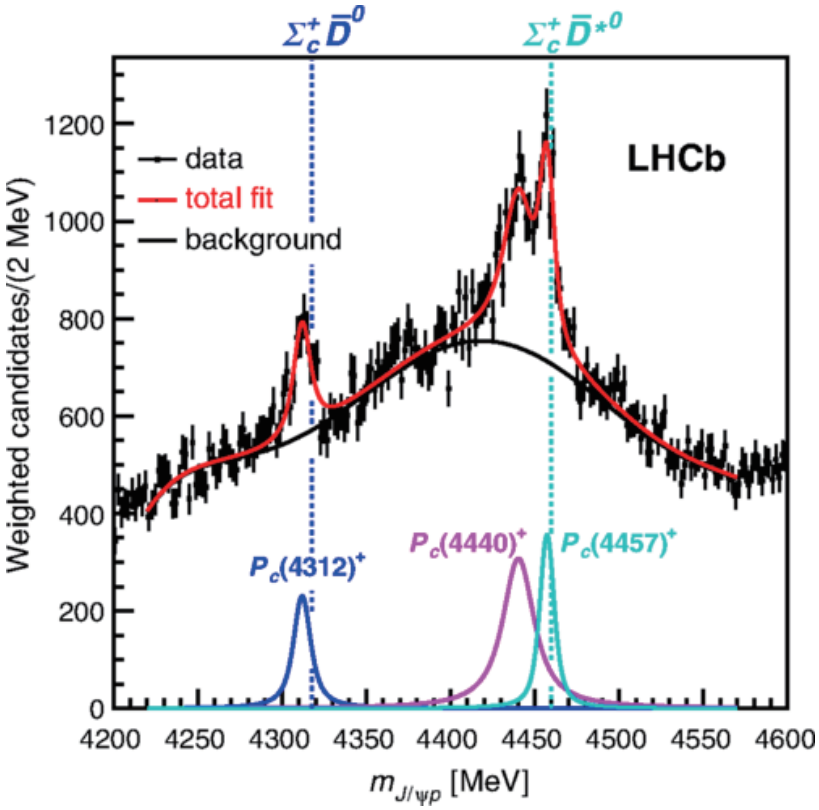

FIG. 1. $J/\psi p$ invariant-mass distribution for the $\Lambda_b \to J/\psi p K^-$ decay taken from Ref. [6]. Three peaks corresponding to pentaquark baryons are observed just below the $\Sigma_c^+ \bar{D}^0$ and $\Sigma_c^+ \bar{D}^{*0}$ thresholds.

bump to the P_c baryons was observed also at ϕ photoproduction on the proton [11–13]. The differential cross section $d\sigma/dt$ at $t = -|t|_{\rm min}$ as a function of the incident photon energy E_γ showed a resonance-like behavior peaked at around 2.0 GeV as shown in Fig. 2. It should be noted that $E_\gamma \approx 2.0$ GeV corresponds to the center-of-mass (CM) energy $W = \sqrt{s} \approx 2.2$ GeV.

A possibility was discussed that a nucleon resonance $N(2080)3/2^-$ (D_{13}) forms this bump [14]. However, it appears only at forward angles [12], indicating that a conventional resonance interpretation seems inappropriate. Alternatively, the ϕ-$\Lambda(1520)$ interference was considered that the final-state K^+K^-p particles are the same between the $\gamma p \to \phi p$ and $\gamma p \to K^+\Lambda(1520)$ reactions. However, the interference effect does not account for the bump since it has been also observed in the neutral mode of ϕ photoproduction ($\gamma p \to K^0_S K^0_L p$) [15] and since the relative phase between ϕ and $\Lambda(1520)$ does not form the bump [16]. As a

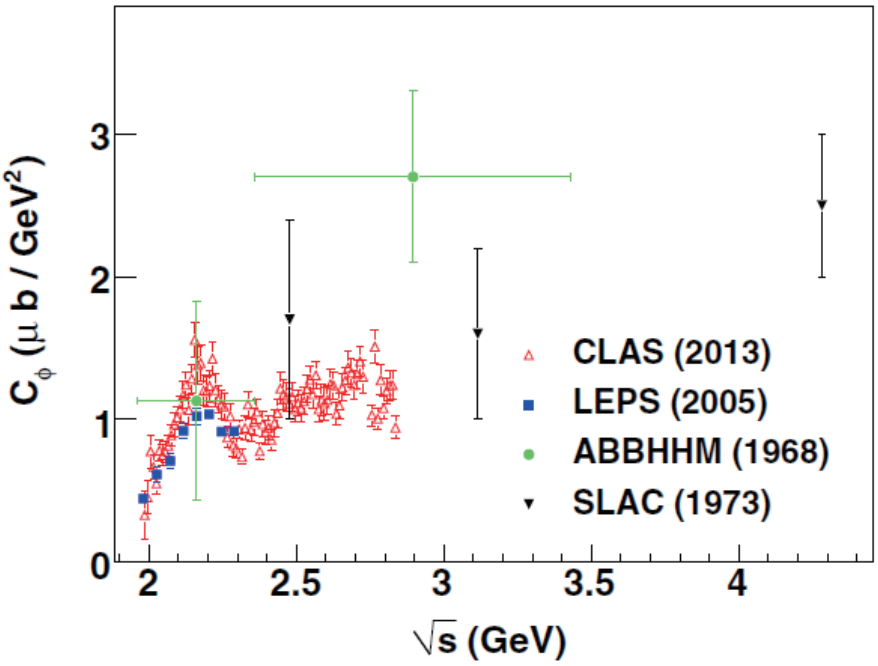

FIG. 2. Differential cross section $d\sigma/dt$ at $t = -|t|_{\rm min}$ as E_γ taken from Ref. [12]. A bump is observed at CM energies around 2.2 GeV.

result of the OZI rule, ϕ photoproduction takes place via a Pomeron trajectory (a multi-gluon exchange) with $J^{PC} = 0^{++}$, showing a monotonically increasing $d\sigma/dt$ at $t = -|t|_{\rm min}$ as a function of E_γ. The bump cannot be reproduced even if incorporated is the non-perturbative two-gluon-exchange dynamics [17] or the manifestation of a daughter Pomeron trajectory [18].

At present, the origin of the bump around $W = 2.2$ GeV in $d\sigma/dt$ at $t = -|t|_{\rm min}$ is not clear. This is partly because the ϕN interaction is not considered to be strong enough producing a resonance except for that in the nuclear medium [19]. Recently, Strakovsky *et al.* extracted the absolute value of the scattering length $|a_{\phi N}| = 0.063 \pm 0.010$ from ϕ photoproduction on the proton ($\gamma p \to \phi p$) near the threshold assuming a vector-meson dominance (VMD) model [20]. The extracted value is consistent with a weak ϕN interaction. More recently, two particle correlation in the pp collision suggests an attractive ϕp interaction [21]. The scattering length $a_{\phi N}$ obtained is $(0.85 \pm 0.34 \pm 0.14) + i\,(0.16 \pm 0.10 \pm 0.09)$ fm in the Lednický-Lyuboshits approach [22], which seems inconsistent with the previous values. Although the strength of the ϕN interaction is still controversial, strong attraction

for producing a resonance might be expected.

Once a conventional resonance interpretation was considered to be inappropriate for the bump observed in photoproduction. However, ϕ photoproduction is insensitive to s-channel ϕ-nucleon resonances. The differential cross section $d\sigma/dt$ at a fixed E_γ shows a strong exponential behavior from the threshold as shown in Fig. 3. Owing to the OZI rule, the dominant mechanism in ϕ photoproduction is a diffractive process where the incident photon is converted into ϕ and elastic ϕ-nucleon scattering occurs via t-channel exchange of some particle. The same mechanism would make J/ψ photoproduction insensitive to the P_c baryons. Therefore, pion-induced phi meson production on the proton ($\pi^- p \to \phi n$) is the best way to study ϕ-nucleon resonances. It should be noted that pion-induced J/ψ production on the proton ($\pi^- p \to J/\psi n$) is also important for understanding the structure of P_c baryons as shown in Section C. The $\pi^- p \to \phi n$ reaction gives relatively uniform angular distributions ($d\sigma/dt$) as shown in the next section, suggesting that the t-channel exchange is highly suppressed. The masses of the P_c baryons are close to the $\Sigma_c^+ \bar{D}^0$ and $\Sigma_c^+ \bar{D}^{*0}$ thresholds, while the bump observed in ϕ photoproduction is close to the $K^+\Lambda(1520)$ and $K^{*+}\Lambda$ thresholds. Thus, studying ϕ-nucleon resonances is important not only for identifying hidden-strangeness exotic baryons but also revealing the structure of the P_c baryons.

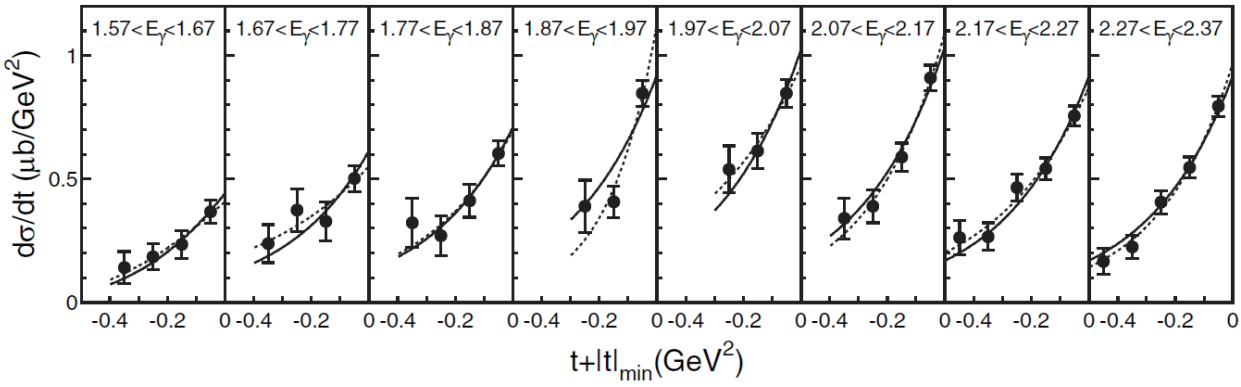

FIG. 3. Differential cross sections $d\sigma/dt'$ for $\gamma p \to \phi p$. The curves show the fitted $d\sigma/dt' = C_\phi \exp(B_\phi t')$ function. The dashed curves show the fitted functions with a free B_ϕ parameter, and the solid with a fixed $B_\phi = 3.38$ GeV$^2/c^2$.

Additionally, $\pi^- p \to \phi n$ is one of the elementary processes of ϕ production. The measured cross sections are an important input for ϕ production in the pA collision for investigating the medium modification of the ϕ properties [23, 24].

II. AVAILABLE $\pi^- p \to \phi n$ DATA

At present, available $\pi^- p \to \phi n$ data are quite limited [25–31]. Table I summarizes the measured total cross sections and number of ϕ- or K^+K^--produced events. Except for Ref. [31], total cross sections were measured before 1980, and their uncertainties are large owing to poor statistics (the number of ϕ- or K^+K^--produced events are much less than 1,000).

TABLE I. Measured total cross sections and number of ϕ- or K^+K^--produced events. At higher incident momenta, large background contribution appears in the K^+K^- invariant mass distribution, the uncertainties of the number of the ϕ-produced events, and those of total cross sections are large.

Reference	P_π (GeV/c)	σ_ϕ (μb)	#events
O.I. Dahl *et al.* (1967) [25]	1.58–1.71	29 ± 15	40 ϕ (84 KK)
	1.8–2.2	30 ± 8	
	2.58–2.63	0 ± 9	
	2.9–3.3	6 ± 8	
	3.8–4.2	15 ± 20	
J.H. Boyd *et al.* (1968) [26]	2.1	10^{+9}_{-8}	95 KK
D. Bollini *et al.* (1969) [27]	2.13	24 ± 8	82 ± 25 ϕ
B.D. Hyams *et al.* (1970) [28]	11.04	$0.128^{+0.027}_{-0.028}$	
D.S. Ayres *et al.* (1974) [29]	3	4.9 ± 2.1	300 ϕ
	4	1.66 ± 0.32	
	5	0.58 ± 0.15	
	6	0.47 ± 0.14	
H. Courant *et al.* (1977) [30]	1.6	19 ± 6	23 ϕ
	1.7	24 ± 7	38 ϕ
	1.8	25 ± 8	80 ϕ
	2.0	21 ± 7	28 ϕ
S.V. Golovskin *et al.* (1997) [31]	32.5	0.0115 ± 0.0033	1670 ± 410 ϕ

It is difficult to investigate the intermediate ϕ-nucleon resonances in detail owing to the lack of total and differential cross-section data in the resonance region ($P_\pi \approx 2$ GeV/c). However, the available data tell us the order of the production cross section. Figure 4 shows the total cross section as a function of the incident pion momentum. The total cross sections are 20–30 μb at $P_\pi \approx 2$ GeV/c although they are not precisely determined. The data also tell us that the t-channel process is highly suppressed at $P_\pi \approx 2$ GeV/c. Figure 5 shows the differential cross section $d\sigma/dt'$ taken from Ref. [29], where t' denotes $t+|t|_{\rm min}$. The B_ϕ slope parameters obtained are 0.4 ± 1.8, 0.1 ± 0.5, 1.2 ± 0.4, and 1.6 ± 0.6 GeV$^2/c^2$ at $P_\pi = 3$, 4, 5, and 6 GeV/c, respectively, when an exponential function $d\sigma/dt' = C_\phi \exp(B_\phi t')$ is fitted to the data. Below $P_\pi = 4$ GeV/c, $d\sigma/dt'$ does not show a strong exponential behavior ($B_\phi \approx 0$), suggesting a rather uniform $d\sigma/d\Omega$ angular distribution in the CM frame. On the contrary, $d\sigma/dt'$ shows a strong exponential behavior (a finite B_ϕ) from the reaction threshold ($E_\gamma = 1.57$ GeV) in photoproduction as shown in Fig. 3. Therefore, the $\pi^- p \to \phi n$ reaction is suitable for studying possible ϕ-nucleon resonances.

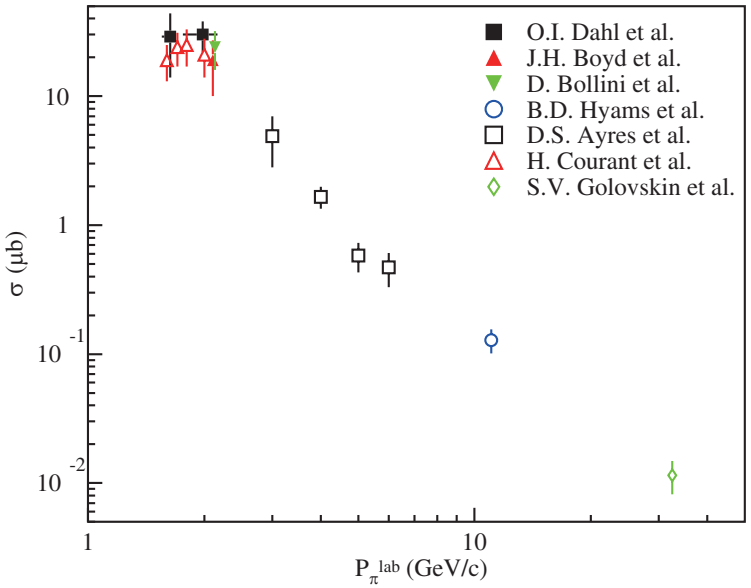

FIG. 4. Total cross section as a function of the incident pion momentum. The cross section data are not precisely determined for the resonance region ($P_\pi \approx 2$ GeV/c) .

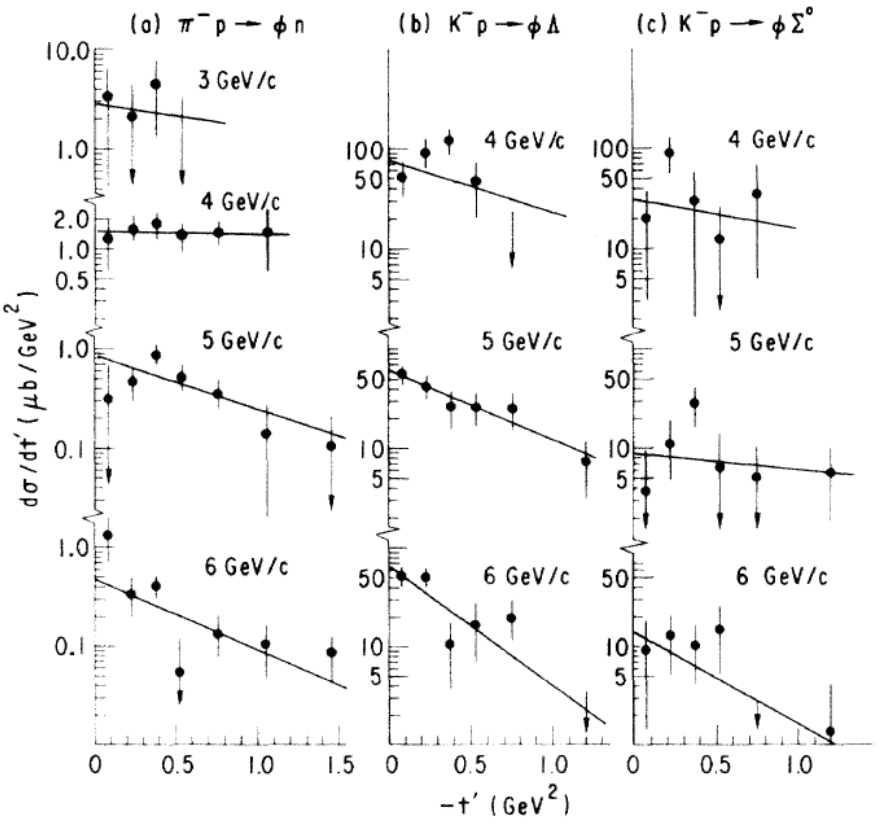

FIG. 5. Differential cross sections $d\sigma/dt'$ for $\pi^- p \to \phi n$ (a) and other reactions taken from Ref. [29]. The lines show the fitted $d\sigma/dt' = C_\phi \exp(B_\phi t')$ function. Here t' denotes $t + |t|_{\rm min}$.

III. KINEMATICS

The ϕ meson has a mass $M = 1019.461 \pm 0.016$ MeV, and a full width $\Gamma = 4.249 \pm 0.013$ MeV [32]. The incident π^- momentum is 1.5593 GeV/c corresponding to the reaction threshold for production of ϕ having the centroid mass. Here, 938.272081, 939.565413, and 139.57039 MeV are employed for masses of the proton, neutron, and charged pion, respectively. At first, we show the CM energy W in Fig. 6(a) as a function of the incident π^- momentum P_π assuming ϕ has its centroid mass. The W increases linearly as increase of P_π. Pion beams at incident momenta of 1.6–2.4 GeV/c provide Ws ranging from 1.96 to 2.33 GeV. We have also estimated the CM-energy coverage ΔW corresponding to momentum bite $\Delta P_\pi/P_\pi = \pm 2\%$ of incident pions as shown in Fig. 6(b). Above 1.6 GeV/c, ΔW also increases linearly as increase of P_π, and ranges from 0.03 to 0.04 GeV.

Next, emitted angles and momenta of ϕs are discussed. Here, the mass of a produced ϕ

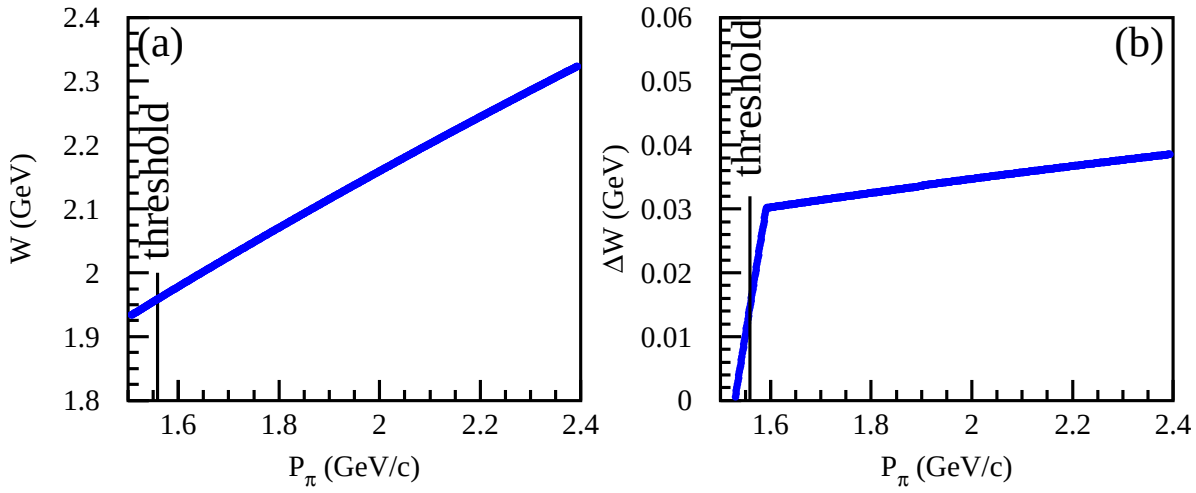

FIG. 6. (a) W as a function of P_π. (b) CM-energy coverage ΔW corresponding to the momentum bite $\Delta p/p = \pm 2\%$ of incident pions as a function of P_π.

meson is determined according to its centroid mass and full width. The generated events are weighted by the phase volume of ϕn production with a certain ϕ mass. Fig 7 shows the momentum P_ϕ as a function of the emitted angle θ_ϕ for ϕs in the laboratory frame. The maximum θ_ϕ increases as increase of P_π. The maximum θ_ϕ is approximately 40° at $P_\pi = 2.4$ GeV/c. The maximum P_ϕ increases and the minimum decreases as increase of P_π. The minimum and maximum P_ϕs are 0.31 and 2.15 GeV/c at $P_\pi = 2.4$ GeV/c. Fig. 8 shows the correlation of θ_ϕs between the CM frame and laboratory frame.

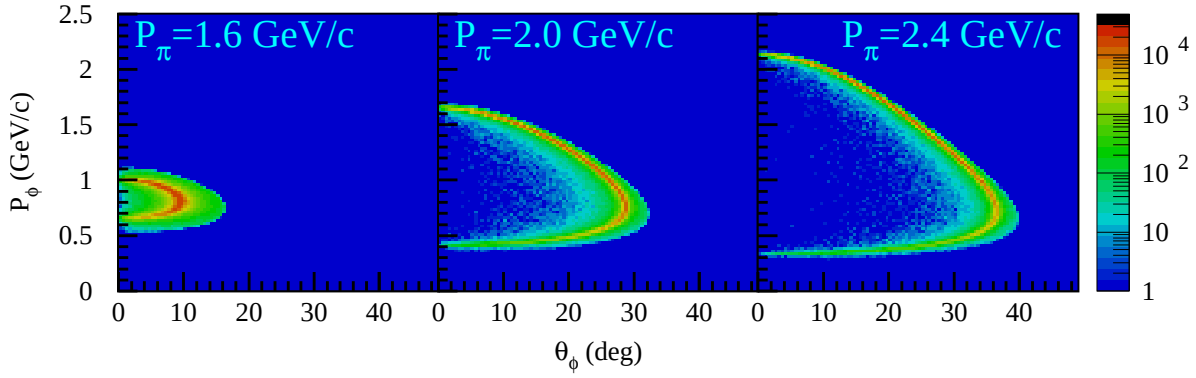

FIG. 7. P_ϕ as a function of θ_ϕ for ϕs in the laboratory frame. At $P_\pi = 2.4$ GeV/c, the maximum θ_ϕ is 40° and the maximum P_ϕ is 2.15 GeV/c.

Finally, we show emitted angles and momenta of kaons to be detected. Here, the generated ϕ meson is assumed to decay isotropically in its rest frame into a K^+K^- pair. Fig. 9

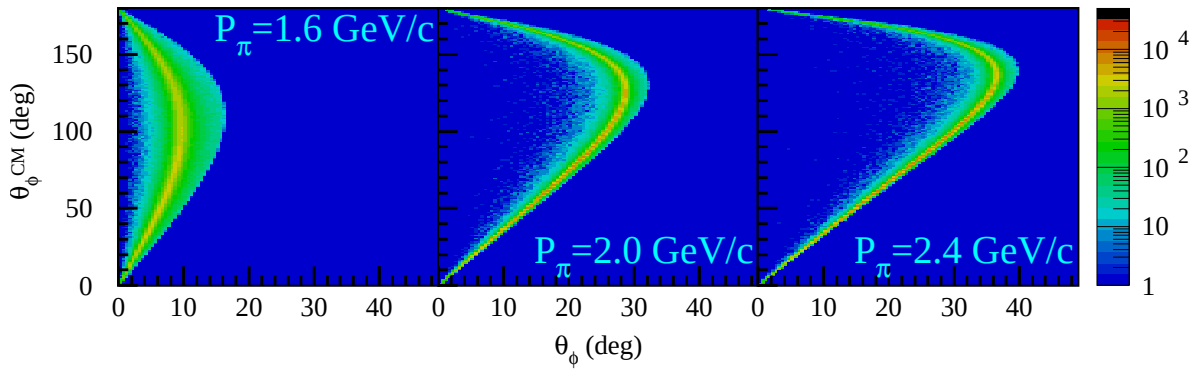

FIG. 8. Correlation of θ_ϕs between the CM frame and laboratory frame. Two θ_ϕs in the CM frame correspond to the same θ_ϕ in the laboratory frame.

shows the K emission angle θ_K as a function of θ_ϕ. The majority of the events makes θ_K proportional to θ_ϕ. This is because the ϕ mass is located near the K^+K^- threshold. The maximum θ_K also increases as increase of P_π. The maximum θ_K is approximately 49°. Fig. 10 shows the K momentum P_K as a function of θ_ϕ. The maximum P_K increases as increase of P_π. The maximum P_K is 1.19 GeV/c at $P_\pi = 2.4$ GeV/c. Figure 11 shows the correlation between P_K and θ_K.

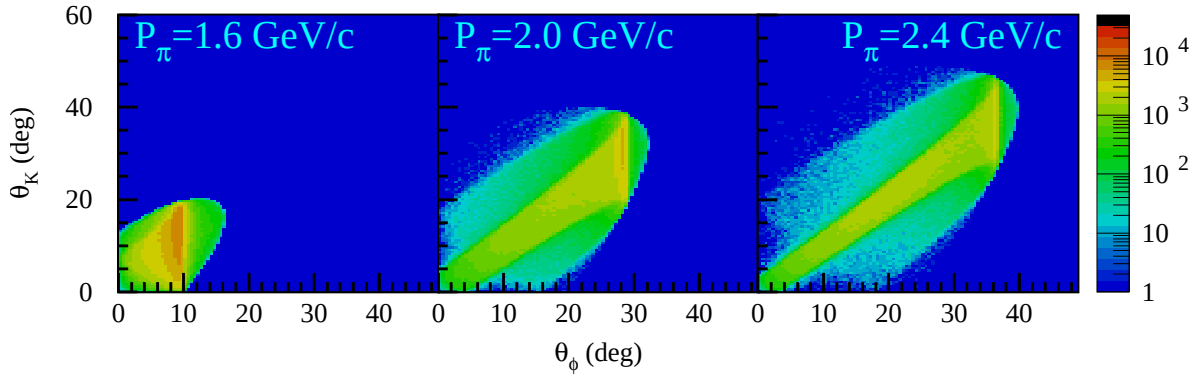

FIG. 9. K emission angle θ_K as a function of θ_ϕ. The majority of the events makes θ_K proportional to θ_ϕ and the maximum θ_K is approximately 49° at $P_\pi = 2.4$ GeV/c.

What we have to do is to detect low-momentum charged kaons emitted at forward angles. It should be noted that the maximum P_K is 1.19 GeV/c and the maximum θ_K is 49.9° in the laboratory frame at $P_\pi \leq 2.4$ GeV/c.

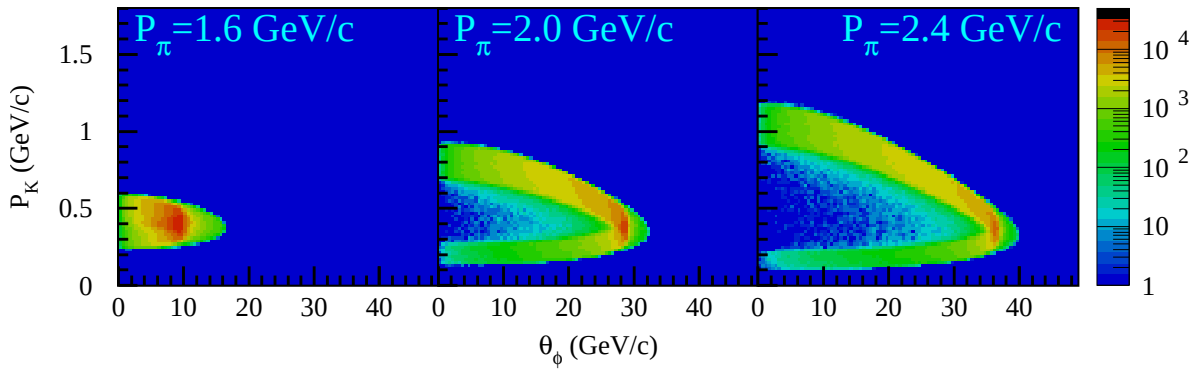

FIG. 10. K momentum P_K as a function of θ_ϕ. The maximum P_K is 1.19 GeV/c at P_π = 2.4 GeV/c.

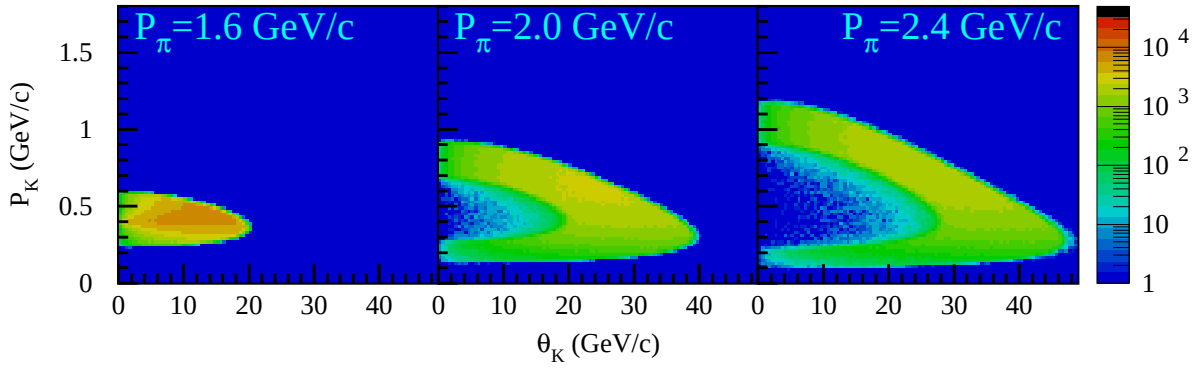

FIG. 11. Correlation between P_K and θ_K. At $P_\pi = 2.4$ GeV/c, the maximum θ_K is approximately 49°, and the maximum P_K is 1.19 GeV/c.

IV. EXPERIMENTAL SETUP

Currently, the E16 experiment uses a 30-GeV primary proton beam at the high-momentum (high-p) beamline at J-PARC. The high-p beamline splits off from the main slow extraction beamline. The septum magnet (SM) for this split is located in the middle of the switchyard for slow extraction. A small fraction of the primary protons ($\approx 10^{10}$ Hz) are delivered at the high-p beamline. Since a production target can be placed at SM with 15-kW loss at maximum, high-intensity secondary pions can be produced and provided in principle at the beamline.

We have a lot of issues to be resolved for providing secondary particles at the high-p beamline fitted to the planned flagship experiment aiming at spectroscopy of charmed

baryons [33]: a production target of secondary particles, polarity change of power supplies for magnets, kicker magnets, swinger magnets upstream and downstream of the production target, radiation shield, and regulations. It is necessary to develop production target which withstands heat from a 15-kW loss of the primary beam. Polarities of power supplies for magnets are currently fixed for the primary proton beam. Polarity-change of the power supplies are required for providing negatively-charged particles. To increase the intensity of secondary particles, collected should be emitted particles at forward angles. For this purpose, we need to place swinger magnets upstream and downstream of the target. Additionally, we need a kicker magnet especially for the vertical direction to collect the secondary particles efficiently. Finally, we need additional radiation shield and new regulations.

Even though we do not place a dedicated production target, the collimator for the Lambertson magnet plays a role as a target for producing secondary particles. In this case, the expected intensity is 3.93, 5.40, 7.05, 8.87, 10.86 kHz at P_π = 1.6, 1.8, 2.0, 2.2, and 2.4 GeV/c, respectively, after optimizing the intensity with a 400-W loss of the primary proton beam without swinger magnets. Figure 12 shows the expected intensity of secondary negatively-charged particles as a function of the momentum. To provide a negative pion

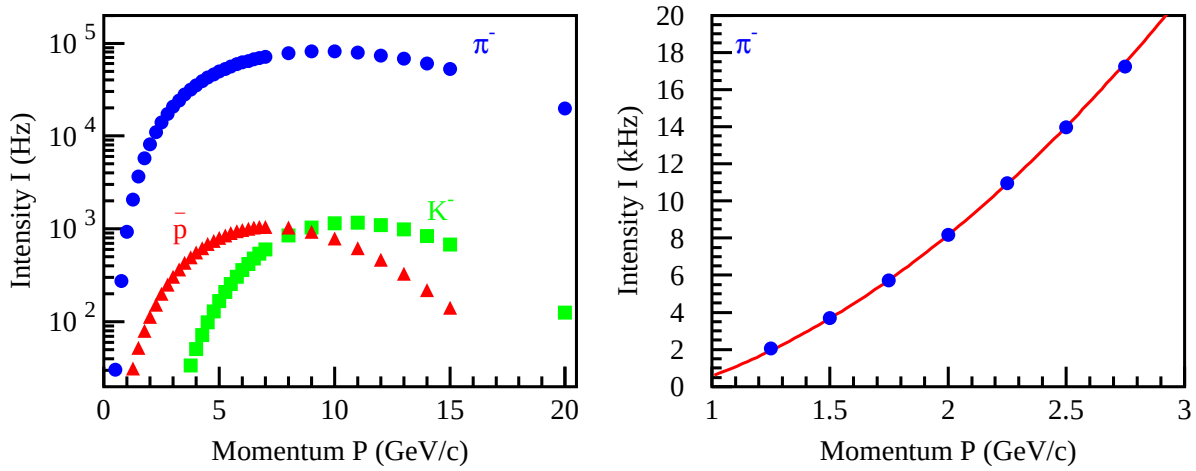

FIG. 12. Expected intensity of secondary negatively-charged particles as a function of the momentum for a 400-W loss of the primary proton beam. The left panel shows the intensities for π^- (blue), K^- (green), and $\bar{p}$ (red) at momenta below 20 GeV/c, and the right panel shows the π^- intensity at momenta ranging from 1 to 3 GeVc. The red curve represents the fitted quadratic function to the data shown in the right panel: $I/\mathrm{kHz} = 2.72\,\{P/\,(\mathrm{GeV}/c)\}^2 - 0.56P/\,(\mathrm{GeV}/c) - 1.61$.

beam, the polarity change is required for power supplies for magnets. To increase the intensity, a kicker magnet for the vertical direction (V20) is also required. We may need to place additional radiation shield, and modify regulations slightly. We can hopefully use negative pions with a momentum of $\approx$ 2 GeV/c and an intensity of $\approx 10^4$ Hz at the 400-W loss, which is enough for studying ϕN resonances via the $\pi^- p \to \phi n$ reaction, just after the long shutdown period (2023–2025).

We plan to use the FM magnet for the E16 spectrometer as shown in Fig. 13. Each pole tip takes a cone shape, and the magnetic flux density at the central region is quite high ($\approx$ 1.8T). Figure 14 shows the magnetic flux density of the FM magnet along z, x, and y axes. Here, the z axis is taken along the central beam direction, and the y axis is defined as the vertical direction.

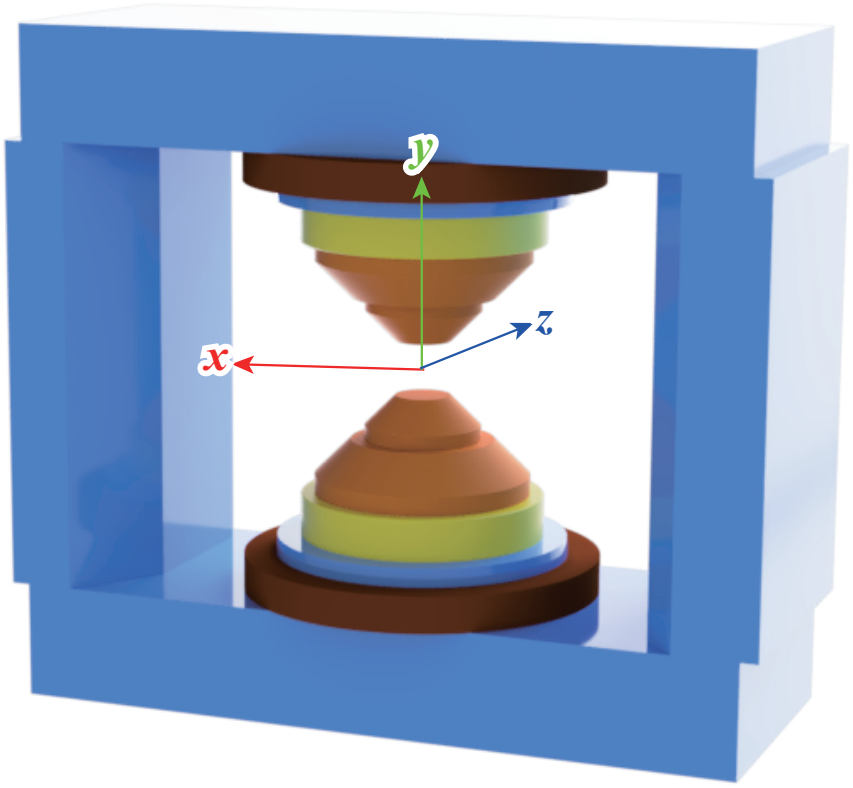

FIG. 13. Schematic view of the FM magnet and the definition of the axes. The z axis is taken along the central beam direction, and the y axis is defined as the vertical direction.

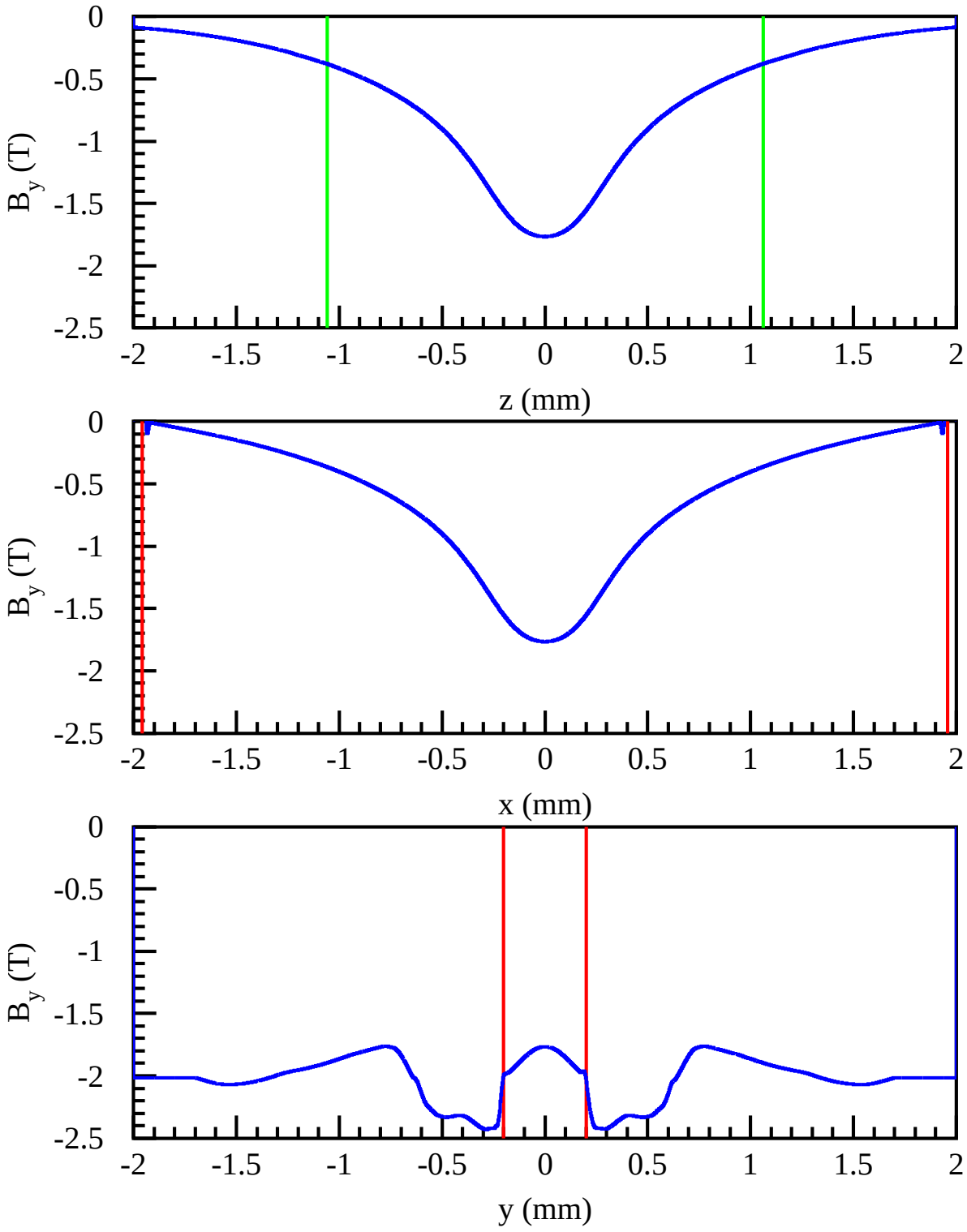

FIG. 14. Magnetic flux density of the FM magnet for the E16 spectrometer along z, x, and y axes. The green lines denote the entrance and exit surface of the yoke, and the red denote the boundaries of the yoke.

We estimate the acceptance of detecting K^+K^- pairs from the ϕ decay for a fixed P_π. We assume ϕs are generated isotropically in the CM frame, and each of them decays isotropically into a K^+K^- pair. Assumed to be detected are K^+s and K^-s coming to a cylindrical region within $|\Psi_h| = |\tan^{-1}(x/z)| < \Psi_h^0$ and $|y| < 0.9$ m at $\sqrt{x^2+y^2} = 1.5$ m. This angular coverage can be realized by combining the current E16 detector system and developing E50 detector system. Figures 15 shows the angular coverage of the detector system for Ψ_h^0. For instance, the forward angles ($|\Psi_h| < 45°$) could be covered by the planar scintillating fiber trackers, drift chambers, and plastic scintillator hodoscopes developed for the E50 experiment, and the backward angles, $45° \leq |\Psi_h| < 75°$, could be covered by the E16 tracking system consisting of silicon-strip detectors (SSDs) and gas electron multipliers (GEMs) together with the resistive-plate chambers (RPCs) developed for the E50 experiment.

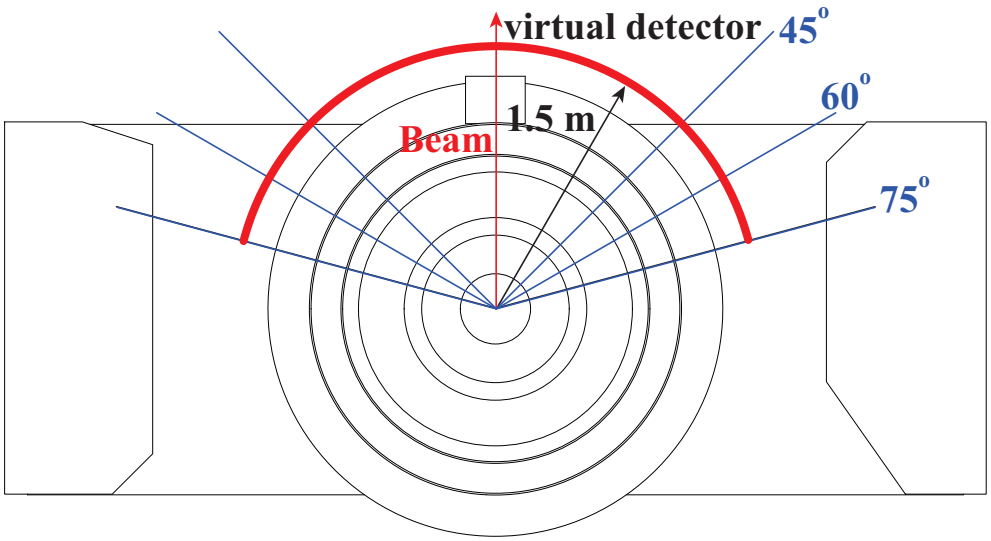

FIG. 15. Angular coverage of the detector system for $\Psi_h^0 = 75°$. We assume the detector covering a cylindrical region within $|\Psi_h| = \left|\tan^{-1}(x/z)\right| < \Psi_h^0$ and $|y| < 0.9$ m at $\sqrt{x^2+y^2} = 1.5$ m.

We estimate the geometrical acceptance, the probability that both K^+ and K^-, which do not decay in flight, arrive at a detector, and the acceptance including the effects of K^+ and K^- decays in flight. Table II summarizes the acceptances of detecting K^+K^- pairs from the ϕ decay for a fixed P_π. In this table, we show the acceptances for the several angular coverages ($\Psi_h^0 = 45°$–$120°$). Since the K^+s and K^-s from the ϕ decays are emitted at forward angles ($\theta_K < 49°$), we can get high geometrical acceptance only covering $|\Psi_h| < 45°$. Some

of the K^+s and K^-s arrive at a detector with $|\Psi_h| \geq 45^\circ$ owing to the magnetic flux density.

TABLE II. Acceptance of detecting K^+K^- pairs from the ϕ decay for a fixed P_π. The acceptance $\mathcal{A}_{\rm geo}$ denotes the probability that both K^+ and K^-, which do not decay in flight, arrive at the detector with a cylindrical region within $|\Psi_h| < \Psi_h^0$ and $|y| < 0.9$ m at $\sqrt{x^2+y^2} = 1.5$ m. Here, Ψ_h denotes $\left|\tan^{-1}(x/z)\right|$, and The acceptance $\mathcal{A}_{\rm det}$ includes the effects of K^+ and K^- decays in flight.

	$\Psi_h^0 = 45^\circ$		$\Psi_h^0 = 60^\circ$		$\Psi_h^0 = 75^\circ$		$\Psi_h^0 = 90^\circ$		$\Psi_h^0 = 105^\circ$		$\Psi_h^0 = 120^\circ$	
P_π	$\mathcal{A}_{\rm geo}$	$\mathcal{A}_{\rm det}$	$\mathcal{A}_{\rm geo}$	$\mathcal{A}_{\rm det}$	$\mathcal{A}_{\rm geo}$	$\mathcal{A}_{\rm det}$	$\mathcal{A}_{\rm geo}$	$\mathcal{A}_{\rm det}$	$\mathcal{A}_{\rm geo}$	$\mathcal{A}_{\rm det}$	$\mathcal{A}_{\rm geo}$	$\mathcal{A}_{\rm det}$
1.6 GeV/c	0.501	0.193	0.818	0.307	0.960	0.352	0.998	0.362	1.000	0.362	1.000	0.362
1.8 GeV/c	0.535	0.249	0.735	0.327	0.845	0.363	0.906	0.379	0.940	0.386	0.956	0.389
2.0 GeV/c	0.526	0.276	0.701	0.349	0.786	0.378	0.837	0.392	0.865	0.398	0.883	0.402
2.2 GeV/c	0.524	0.300	0.674	0.365	0.748	0.392	0.790	0.404	0.815	0.410	0.831	0.413
2.4 GeV/c	0.527	0.320	0.662	0.383	0.730	0.409	0.762	0.419	0.782	0.424	0.793	0.426

Although the acceptance increases as increase of Ψ_h^0, $\Psi_h^0 = 75^\circ$ seems to provide enough high geometrical acceptance. Thus, we set $\Psi_h^0 = 75^\circ$ and we estimate the acceptance as a function of the ϕ-emission angle. Fig. 16 shows the acceptance of detecting K^+K^- pairs from the ϕ decay as a function of the ϕ-emission angle θ_ϕ for several P_πs.

V. YIELD ESTIMATION

We plan to use negative pion beams at incident momenta ranging from 1.6 to 2.4 GeV/c with a 0.1 GeV/c step. The total cross section assumed here is 20 μb. The target planned to be used is liquid deuterium with a thickness of 10 cm equivalent to approximately 0.45 b^{-1}. The branching ratio of the $\phi \to K^+K^-$ decay is 49.2% $\pm$ 0.5%. The secondary beam extraction is made for the 2-s duration of every 5.2 s cycle, giving the duty factor is 0.385. If 10-kHz pions are provided as a beam, we obtain 660 ϕ-produced events a day. The momentum bite is approximately $\pm$2%, corresponding to ΔW = 0.03–0.04 GeV. The number of $\phi \to K^+K^-$-produced events for a W bin of 10 MeV in a day ranges from 160 to 220 depending on P_π. Since the acceptance is 0.35–0.41 including the effects of

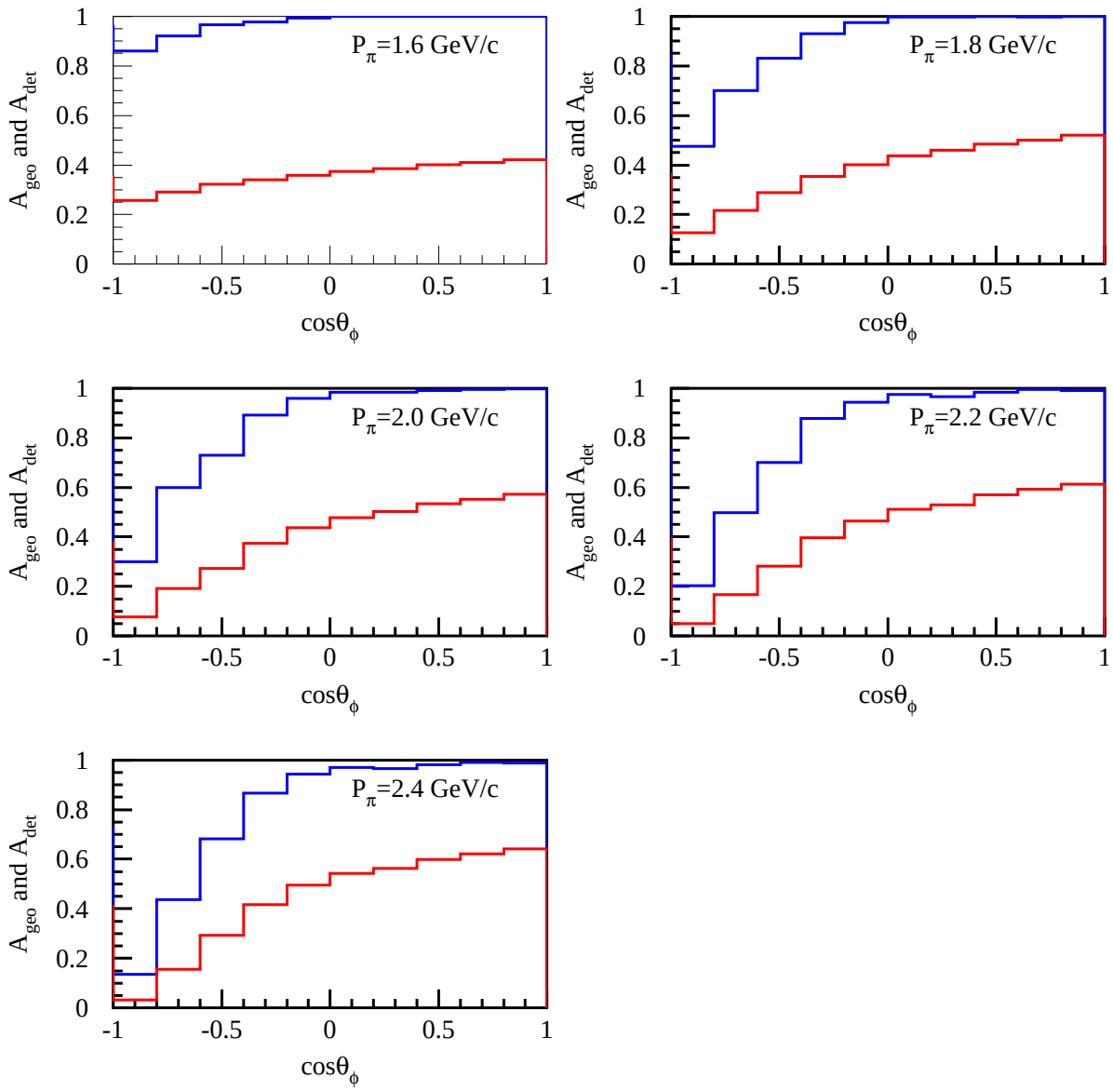

FIG. 16. Acceptance of detecting K^+K^- pairs from the ϕ decay as a function of the ϕ-emission angle θ_ϕ for several P_πs. The blue histograms show the geometrical acceptance $\mathcal{A}_{\rm geo}$ and the red the acceptance $\mathcal{A}_{\rm det}$ including the effects of K^+ and K^- decays in flight.

K^+ and K^- decays in flight, 10-days measurement for each P_π gives approximately several hundred events for each 10-MeV W bin. Table III summarizes the estimated number of the ϕ-produced events in a 10-MeV W bin for 10-days measurement.

Since the maximum intensity of the pion beam is $\approx$ 10 kHz, the hadron reaction rate is expected to be $\approx$ 0.2 kHz assuming the pion-nucleon total cross section of 40 mb. Thus, we can loose the trigger condition for data acquisition, which only requires two charged particle

TABLE III. Estimated number of the ϕ-produced events N_ϕ in a 10-MeV W bin for 10-days measurement. Here, K^+ and K^- are detected without decaying in flight at 1.5-m downstream of the target center. The P_π, I_π, ΔW, and $\mathcal{A}_{\rm det}$ denote the central incident pion momentum, the corresponding intensity of the pion beam for the 400-W loss, W coverage for a given P_π, and the acceptance including the survival ratios of K^+ and K^-.

P_π	I_π	ΔW	$\mathcal{A}_{\rm det}$	N_ϕ
1.6 GeV/c	3.93	30.2 MeV	0.352	300
1.8 GeV/c	5.40	32.5 MeV	0.363	400
2.0 GeV/c	7.05	34.7 MeV	0.378	510
2.2 GeV/c	8.87	36.7 MeV	0.392	630
2.4 GeV/c	10.86	38.7 MeV	0.409	760

detection, or single $K^\pm$ detection, and so on.

VI. SUMMARY

Not clear is the origin of a resonance-like behavior at the CM energy of 2.2 GeV observed in the differential cross section $d\sigma/dt$ at $t = -|t|_{\rm min}$ as a function of the incident photon energy E_γ for ϕ photoproduction on the proton ($\gamma p \to \phi p$). The $d\sigma/dt$ at a fixed E_γ in $\gamma p \to \phi p$ shows a strong exponential behavior from the threshold, suggesting ϕ photoproduction is insensitive to s-channel ϕ-nucleon resonances. To reveal the origin of this bump, we would like to measure the angular differential cross section $d\sigma/d\Omega$ for pion-induced phi meson production on the proton ($\pi^- p \to \phi n$) at incident pion momenta ranging from 1.6 to 2.4 GeV/c. We plan to use secondary pions ($\approx$ 10 kHz) delivered at the high-p beamline with a 400-W loss of the primary proton beam at the Lambertson magnet. We utilize the E16 spectrometer magnet and the combined detector system of E16 and E50, which provides high geometrical acceptance of detecting a K^+ and K^- pair from the ϕ decay. We expect to obtain several hundred ϕ-produced events at a fixed incident momentum in 10-days measurement. We could confirm whether the same bump is observed in $\pi^- p \to \phi n$ or not from five sets of 10-days measurement (P_π = 1.6, 1.8, 2.0, 2.2, 2.4 GeV/c).

Appendix A: Exchange particle in $\pi^- p \to \phi n$ at high incident momenta

At high incident momenta, the dominant production mechanism of pion-induced ϕ production is t-channel exchange of some particle. Figure 17 shows the expected dominant diagram for $\pi^- p \to \phi n$. The negatively-charged pion (π^-) and ρ^- meson are candidates of the exchange particle for this reaction. Since the branching ratio of the $\phi \to \rho\pi$ decay ($\approx 15\%$ including the $\phi \to \pi^+\pi^-\pi^0$ decay) is much larger than that of the $\phi \to \pi^+\pi-$ decay ($\approx 10^{-4}\%$) [32]. The ρ^- is considered to be a dominant contributor for exchange particles.

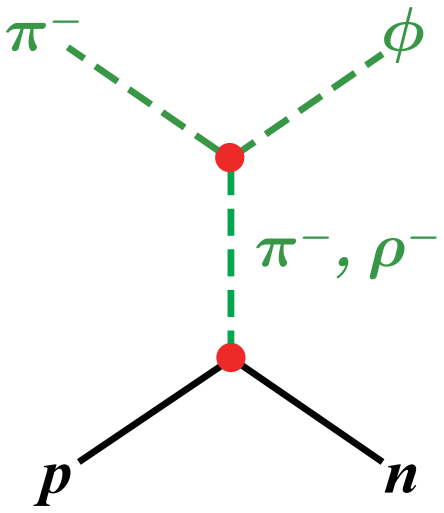

FIG. 17. Expected dominant diagram for $\pi^- p \to \phi n$ at high incident momenta. The π^- and ρ^- are candidates of the exchange particle.

Nevertheless, the main contribution does not come from ρ^- exchange. Table **??** summarizes some elements of the spin-density matrix in the helicity frame for $\pi^- p \to \phi n$. The elements of the spin density matrix ρ_{ij} of ϕ in $\pi^- p \to \phi n$ are described in the next section. Although the natural-parity exchange is expected owing to the nature of ρ, small is the sum of the two elements $\rho_{11} + \rho_{1-1}$ corresponding to the natural-parity exchange. Additionally, a sizable ρ_{00} and a large $\rho_{11} - \rho_{1-1}$ suggest the large contribution of the unnatural-parity exchange. There is a possibility that the elements indicating unnatural-parity exchange come from the effects of s-channel and that more ρ exchange takes place at higher incident momenta since $\rho_{11} + \rho_{1-1}$ increases and $\rho_{11} - \rho_{1-1}$ decreases with increase of incident pion momentum. Or other particle such as $b_1(1235)$ possibly having the $s\bar{s}$ component could play

a dominant role in t-channel exchange since neither π nor ρ has $s\bar{s}$ component.

TABLE IV. Elements of the spin-density matrix of ϕ in the helicity frame for $\pi^- p \to \phi n$ taken from Ref. [29].

P_π	$-t'$	$\rho_{11}+\rho_{1-1}$	ρ_{00}	$\rho_{11}-\rho_{1-1}$	Re[ρ_{10}]
4 GeV/c	0.15–0.90 GeV$^2/c^2$	0.12 ± 0.14	0.26 ± 0.17	0.61 ± 0.17	0.14 ± 0.10
5 and 6 GeV/c (average)	0.15–0.90 GeV$^2/c^2$	0.38 ± 0.08	0.20 ± 0.09	0.43 ± 0.09	0.06 ± 0.05

Appendix B: Spin density matrix of ϕ in $\pi^- p \to \phi n$

Ref. [36] provides the formalism to analyze vector meson production with polarized photons in detail. Here, spin density matrix (SDM) of ϕ is given for $\pi^- p \to \phi n$. The π is a spinless particle giving only one SDM element $\rho_{00} = 1$. The polarization state of ϕ is expressed in terms of its spin space density matrix $\rho(\phi)$, which is connected by the production amplitudes T:

$$\rho(\phi) = T\rho(\pi)T^\dagger. \tag{B1}$$

In the helicity frame, SDM of ϕ is described in the following equation:

$$\rho_{\lambda_\phi \lambda'_\phi}(\phi) = \frac{1}{N} \sum_{\lambda_n \lambda_p} T_{\lambda_\phi \lambda_n, 0\lambda_p} \rho_{00}(\pi) T^*_{\lambda'_\phi \lambda_n, 0\lambda_p} \tag{B2}$$

where λs denotes the helicities of the respective particles of the $\pi^- p \to \phi n$ reaction, and N is the normalization factor:

$$N = \frac{1}{2} \sum_{\lambda_\phi, \lambda_n, \lambda_p} \left| T_{\lambda_\phi \lambda_n, 0\lambda_p} \right|^2. \tag{B3}$$

The normalization of T is chosen so that the production cross section is given by

$$\frac{d\sigma}{d\Omega} = \left(\frac{2\pi}{k}\right)^2 \frac{1}{2} \sum_{\lambda_\phi, \lambda_n, \lambda_p} \left| T_{\lambda_\phi \lambda_n, 0\lambda_p} \right|^2 \tag{B4}$$

where k denotes the incident pion momentum.

We consider the $\phi \to K^+K^-$ decay where a vector meson decays into two spinless particles. The decay angular distribution of Ks from the ϕ-decay is discussed in the helicity of ϕ. The z direction is chosen opposite to the direction of the outgoing neutron n in the rest

system of ϕ. The y direction is the normal to the production plane, defined by the cross product $\hat{k} \times \hat{q}$ of the three-momenta $\hat{k}$ of the incident π and that $\hat{q}$ of the produced ϕ. The x direction is given by $\hat{x} = \hat{y} \times \hat{z}$. The decay angles θ and ϕ of K corresponding to the momentum direction $\hat{\pi}$ are defined as the polar and azimuthal angles of Ks in the rest frame of ϕ. The θ and ϕ for giving the decay angles satisfy

$$\begin{aligned} \cos\theta &= \hat{\pi} \cdot \hat{z}, \\ \cos\phi &= -\frac{\hat{y} \cdot (\hat{z} \times \hat{\pi})}{|\hat{z} \times \hat{\pi}|}, \text{ and} \\ \sin\phi &= -\frac{\hat{x} \cdot (\hat{z} \times \hat{\pi})}{|\hat{z} \times \hat{\pi}|}. \end{aligned} \tag{B5}$$

The decay angular distribution of K in the rest frame of ϕ reads:

$$W(\theta, \phi) \equiv \frac{dN}{d\cos\theta\, d\phi} = \sum_{\lambda_\phi, \lambda'_\phi} \langle \theta, \phi \,|M|\, \lambda_\phi \rangle\, \rho_{\lambda_\phi, \lambda'_\phi} \left\langle \lambda'_\phi \,|M^*|\, \theta, \phi \right\rangle \tag{B6}$$

where M is the decay amplitude:

$$\langle \theta, \phi \,|M|\, \lambda_\phi \rangle = C \sqrt{\frac{3}{4\pi}} D^{1*}_{\lambda_\phi 0}(\phi, \theta, -\phi)\,. \tag{B7}$$

The quantity $|C|^2$ is proportional to the decay width of ϕ. We consider a normalized decay angular distribution, we chose $C = 1$. The Wigner rotation function D is given by

$$\begin{aligned} D^1_{10}(\phi, \theta, -\phi) &= -\frac{1}{\sqrt{2}} \sin\theta \exp(-i\phi)\,, \\ D^1_{00}(\phi, \theta, -\phi) &= \cos\theta, \text{ and} \\ D^1_{-10}(\phi, \theta, -\phi) &= +\frac{1}{\sqrt{2}} \sin\theta \exp(+i\phi)\,. \end{aligned} \tag{B8}$$

The decay angular distribution (B6) can be written as

$$W(\theta, \phi) = \frac{3}{4\pi} \sum_{\lambda_\phi, \lambda'_\phi} D^{1*}_{\lambda_\phi 0}(\phi, \theta, -\phi)\, \rho(\phi)_{\lambda_\phi, \lambda'_\phi} D^1_{\lambda'_\phi 0}(\phi, \theta, -\phi)\,. \tag{B9}$$

Using the fact that the $\rho(\phi)$ is hermitian, $\rho(\phi)_{\lambda_\phi, \lambda'_\phi} = \rho^*(\phi)_{\lambda'_\phi, \lambda_\phi}$, we obtain

$$\begin{aligned} W(\theta, \phi) = \frac{3}{4\pi} \Big\{ & \frac{1}{2}(\rho_{11} + \rho_{-1-1}) \sin^2\theta + \rho_{00} \cos^2\theta \\ & + \frac{1}{\sqrt{2}} (-\mathrm{Re}[\rho_{10}] + \mathrm{Re}[\rho_{-10}]) \sin 2\theta \cos\phi \\ & + \frac{1}{\sqrt{2}} (\mathrm{Im}[\rho_{10}] + \mathrm{Im}[\rho_{-10}]) \sin 2\theta \sin\phi \\ & - \mathrm{Re}[\rho_{1-1}] \sin^2\theta \cos 2\phi + \mathrm{Im}[\rho_{1-1}] \sin^2\theta \cos 2\phi \Big\} \end{aligned} \tag{B10}$$

Now, let's discuss separation of natural- and unnatural-parity exchange contributions using the symmetry properties of the helicity amplitudes:

$$T_{-\lambda_\phi-\lambda_n,-\lambda_\pi-\lambda_p} = (-1)^{\left(\lambda_\phi-\lambda_n\right)-(\lambda_\pi-\lambda_p)} T_{\lambda_\phi\lambda_n,\lambda_\pi\lambda_p}, \tag{B11}$$

where $\lambda_\pi = 0$ because π^- is a spinless particle. Considering pure t-channel exchange of a particle with a spin-parity of J^π,

$$T_{-\lambda_\phi\lambda_n,-\lambda_\pi\lambda_p} = \pi\pi_\phi\pi_\pi(-1)^{J+J_\phi-J_\pi+\lambda_\phi-\lambda_\pi} T_{\lambda_\phi\lambda_n,\lambda_\pi\lambda_p}. \tag{B12}$$

Hence, the production amplitude for the natural-parity exchange reads:

$$T^N_{-\lambda_\phi\lambda_n,0\lambda_p} = -(-1)^{\lambda_\phi} T^N_{\lambda_\phi\lambda_n,0\lambda_p}, \text{ and} \tag{B13}$$

that for the unnatural-parity exchange reads:

$$T^U_{-\lambda_\phi\lambda_n,0\lambda_p} = +(-1)^{\lambda_\phi} T^U_{\lambda_\phi\lambda_n,0\lambda_p}. \tag{B14}$$

From Eqs. (B13) and (B14), the following projection relations are obtained:

$$\begin{aligned} T^N_{\lambda_\phi\lambda_n,0\lambda_p} &= \frac{1}{2}\left(T_{\lambda_\phi\lambda_n,0\lambda_p} - (-1)^{\lambda_\phi} T_{-\lambda_\phi\lambda_n,0\lambda_p}\right), \text{ and} \\ T^U_{\lambda_\phi\lambda_n,0\lambda_p} &= \frac{1}{2}\left(T_{\lambda_\phi\lambda_n,0\lambda_p} + (-1)^{\lambda_\phi} T_{-\lambda_\phi\lambda_n,0\lambda_p}\right). \end{aligned} \tag{B15}$$

Thus, the parity conservation reduces the number of independent matrix elements

$$\rho_{\lambda\lambda'} = (-1)^{\lambda-\lambda'}\rho_{-\lambda-\lambda'}. \tag{B16}$$

Using $\rho_{-1-1} = \rho_{11}$ and $\mathrm{Im}[\rho_{1-1}] = 0$, the decay angular distribution (B10) reads:

$$\begin{aligned} W(\theta,\phi) = \frac{3}{4\pi}\Big\{ & \rho_{00}\cos^2\theta + (\rho_{11}-\rho_{1-1})\sin^2\theta\cos^2\phi \text{ [unnatural-parity exchange]} \\ & + (\rho_{11}+\rho_{1-1})\sin^2\theta\sin^2\phi \text{ [natural-parity exchange]} \\ & - \sqrt{2}\mathrm{Re}[\rho_{10}]\sin 2\theta\cos\phi\Big\}. \end{aligned} \tag{B17}$$

The $\rho_{11}+\rho_{1-1}$ corresponds to the natural-parity exchange contribution, and the ρ_{00} and $\rho_{11}-\rho_{1-1}$ provide the unnatural-parity exchange.

Appendix C: Study of P_c baryons via $\pi^- p \to J/\psi n$

Recently, the LHCb collaboration observed exotic hidden-charm P_c baryons, $P_c(4312)^+$, $P_c(4440)^+$, and $P_c(4457)^+$ in the $J/\psi p$ invariant-mass distributions for the $\Lambda_b \to J/\psi p K^-$ decay [5, 6]. The structure of this If a P_c baryon really exists, it should show up independently of the initial state of reactions. However, corresponding peaks are not observed in the total cross section measured by the GlueX collaboration as a function of the incident photon energy for J/ψ photoproduction on the proton ($\gamma p \to J/\psi p$). Still not definitely settled is what is the structure of the P_c baryons [8–10]. Similarly to $\gamma p \to \phi p$, $\gamma p \to J/\psi p$ is insensitive to s-channel $J/\psi p$ resonances. It is very important to confirm these P_c baryons in other possible reactions such as $\pi^- p \to J/\psi n$ which is expected to be much more sensitive to s-channel $J/\psi p$ resonances. In Ref. [35], the total cross section predicted is 1 nb near the P_c masses for $\pi^- p \to J/\psi n$, while that for the background processes is the order of 10^{-4}–10^{-3} nb. In Ref. [34], the total cross section is 1 μb . Although it is much larger than that in Ref. [35], it is still small to produce J/ψs with $\approx$ 100-kHz pion beams. When we get higher intensity pion beam and a dedicated system for detecting J/ψ, we should measure the cross sections for $\pi^- p \to J/\psi n$.

---

[1] F. E. Close, *"An Introduction to Quarks and Partons,"* Academic Press, 1979.

[2] A. Hosaka and H. Toki, *"Quarks, baryons and chiral symmetry,"* World Scientific, 2001.

[3] M. Oka and K. Yazaki, *"Short Range Part of Baryon Baryon Interaction in a Quark Model. 1. Formulation,"* Prog. Theor. Phys. **66**, 556–571 (1981).

[4] M. Oka and K. Yazaki, *"Short Range Part of Baryon Baryon Interaction in a Quark Model. 2. Numerical Results for S-Wave,"* Prog. Theor. Phys. **66**, 572–587 (1981).

[5] R. Aaij *et al.* (LHCb collaboration), *"Observation of $J/\psi p$ Resonances Consistent with Pentaquark States in $\Lambda_b^0 \to J/\psi K^- p$ Decays,"* Phys. Rev. Lett. **115**, 072001 (2015).

[6] R. Aaij *et al.* (LHCb collaboration), *"Observation of a narrow pentaquark state, $P_c(4312)^+$, and of two-peak structure of the $P_c(4450)^+$,"* Phys. Rev. Lett. **122**, 222001 (2019).

[7] A. Ali *et al.* (GlueX collaboration), *"First Measurement of Near-Threshold J/ψ Exclusive Photoproduction off the Proton,"* Phys. Rev. Lett. **123**, 072001 (2019).

[8] H. X. Chen, W. Chen, X. Liu and S. L. Zhu, *"The hidden-charm pentaquark and tetraquark states,"* Phys. Rept. **639**, 1–121 (2016).

[9] A. Esposito, A. Pilloni and A. D. Polosa, *"Multiquark Resonances,"* Phys. Rept. **668**, 1–97 (2017).

[10] A. Ali, J. S. Lange and S. Stone, *"Exotics: Heavy Pentaquarks and Tetraquarks,"* Prog. Part. Nucl. Phys. **97**, 123–198 (2017).

[11] T. Mibe *et al.* (LEPS collaboration), *"Diffractive phi-meson photoproduction on proton near threshold,"* Phys. Rev. Lett. **95**, 182001 (2005).

[12] B. Dey *et al.* (CLAS collaboration), *"Data analysis techniques, differential cross sections, and spin density matrix elements for the reaction $\gamma p \to \phi p$,"* Phys. Rev. C **89**, 055208 (2014).

[13] K. Mizutani *et al.* (LEPS collaboration), *"ϕ photoproduction on the proton at E_γ = 1.5–2.9 GeV,"* Phys. Rev. C **96**, 062201 (2017).

[14] A. Kiswandhi, J. J. Xie and S. N. Yang, *"Is the nonmonotonic behavior in the cross section of phi photoproduction near threshold a signature of a resonance?,"* Phys. Lett. B **691**, 214–218 (2010).

[15] H. Seraydaryan *et al.* (CLAS collaboration), *"ϕ-meson photoproduction on Hydrogen in the neutral decay mode,"* Phys. Rev. C **89**, 055206 (2014).

[16] S. Y. Ryu *et al.* (LEPS collaboration), *"Interference effect between ϕ and $\Lambda(1520)$ production channels in the $\gamma p \to K^+K^-p$ reaction near threshold,"* Phys. Rev. Lett. **116**, 232001 (2016).

[17] A. I. Titov and T. S. H. Lee, *"Spin effects and baryon resonance dynamics in phi meson photoproduction at few GeV,"* Phys. Rev. C **67**, 065205 (2003).

[18] T. Nakano and H. Toki, *"Glueball hunt in Phi photoproduction,"* in proceedings of the 5th Tamura Symposium: International Workshop on Exciting Physics with New Accelerators Facilities (EXPAF 97), 48–54 (1997).

[19] T. Ishikawa, D. S. Ahn, J. K. Ahn, H. Akimune, W. C. Chang, S. Date, H. Fujimura, M. Fujiwara, K. Hicks and T. Hotta, *et al. "ϕ photo-production from Li, C, Al, and Cu nuclei at $E_\gamma = 1.5$–2.4 GeV,"* Phys. Lett. B **608**, 215-222 (2005).

[20] I. I. Strakovsky, L. Pentchev and A. Titov, *"Comparative analysis of ωp, ϕp, and $J/\psi p$ scattering lengths from A2, CLAS, and GlueX threshold measurements,"* Phys. Rev. C **101**, 045201 (2020).

[21] S. Acharya *et al.* (ALICE collaboration), *"Experimental Evidence for an Attractive p-ϕ Interaction,"* Phys. Rev. Lett. **127**, 172301 (2021).

[22] R. Lednický and V. L. Lyuboshits, *"Final State Interaction Effect on Pairing Correlations Between Particles with Small Relative Momenta,"* Yad. Fiz. **35**, 1316-1330 (1981).

[23] R. Muto *et al.* [KEK-PS-E325], Phys. Rev. Lett. **98**, 042501 (2007) doi:10.1103/PhysRevLett.98.042501 [arXiv:nucl-ex/0511019 [nucl-ex]].

[24] S. Yokkaichi, H. En᾽yo, M. Naruki, R. Muto, T. Tabaru, K. Ozawa, H. Hamagaki, K. Shigaki, S. Sawada, M. Sekimoto *et al.*, "Electron pair spectrometer at the J-PARC 50-GeV PS to explore the chiral symmetry in QCD," Proposals for Nuclear and Particle Physics Experiments at J-PARC, KEK/J-PARC-PAC 2006-06 (2006).

[25] O. I. Dahl, L. M. Hardy, R. I. Hess, J. Kirz and D. H. Miller, *"Strange-particle production in π^- p interactions from 1.5 to 4.2 BeV/c. 1. Three-and-more-body final states,"* Phys. Rev. **163**, 1377-1429 (1967).

[26] J. H. Boyd, A. R. Erwin, W. D. Walker, and E. West, *"Study of $\pi^- p \to \omega n, \phi n$ at 2.10 BeV/c,"* Phys. Rev. **166**, 1458–1472 (1968).

[27] D. Bollini, A. Buhler-Broglin, P. Dalpiaz, T. Massam, F. Navach, F. L. Navarria, M. A. Schneegans and A. Zichichi, *"A measurement of the ϕ-meson production cross-section in $\pi^- p$ interactions at 2.13 GeV/c,"* Il Nuovo Cimento A **60**, 541–554 (1969).

[28] B. D. Hyams, W. Koch, D. C. Potter, L. Von Lindern, E. Lorenz, G. Luetjens, U. Stierlin and P. Weilhammer, *"The reaction $\pi^- p \to K^+ K^- n$ between 988 and 1100 MeV invariant KK mass,"* Nucl. Phys. B **22**, 189–204 (1970).

[29] D. S. Ayres, R. Diebold, A. F. Greene, S. L. Kramer, J. S. Levine, A. J. Pawlicki and A. B. Wicklund, *"ϕ Meson Production in $\pi^- p$ and $K^- p$ Interactions from 3-GeV/c to 6-GeV/c,"* Phys. Rev. Lett. **32**, 1463 (1974).

[30] H. Courant, Y. I. Makdisi, M. L. Marshak, E. A. Peterson, K. Ruddick and J. Smith-Kintner, *"ϕ Production in pi$^-$p Collisions Near Threshold,'* Phys. Rev. D **16**, 1-6 (1977).

[31] S. V. Golovkin, A. P. Kozhevnikov, V. P. Kubarovsky, A. I. Kulyavtsev, V. F. Kurshetsov, L. G. Landsberg, V. V. Molchanov, V. A. Mukhin, I. N. Nikitin and V. I. Solyanik, *et al. "Study of the OZI selection rule in hadronic processes,"* Z. Phys. A **359**, 435–444 (1997).

[32] P. A. Zyla *et al.* [Particle Data Group], *"Review of Particle Physics,"* PTEP **2020**, 083C01 (2020).

[33] H. Noumi, Y. Morino, T. Nakano, K. Shirotori, Y. Sugaya, T. Yamaga, K. Ozawa, T. Ishikawa, Y. Miyachi and K. Tanida, "Charmed Baryon Spectroscopy via the (π^-, D^{*-}) reaction," Proposals for Nuclear and Particle Physics Experiments at J-PARC, KEK/J-PARC-PAC 2012-19 (2013).

[34] Q. F. Lü, X. Y. Wang, J. J. Xie, X. R. Chen and Y. B. Dong, *"Neutral hidden charm pentaquark states $P_c^0(4380)$ and $P_c^0(4450)$ in $\pi^- p \to J/\psi n$ reaction,"* Phys. Rev. D **93**, 034009 (2016).

[35] S. H. Kim, H. C. Kim and A. Hosaka, *"Heavy pentaquark states $P_c(4380)$ and $P_c(4450)$ in the J/ψ production induced by pion beams off the nucleon,"* Phys. Lett. B **763**, 358–364 (2016).

[36] K. Schilling, P. Seyboth and G. E. Wolf, *"On the Analysis of Vector Meson Production by Polarized Photons,"* Nucl. Phys. B **15**, 397–412 (1970).